ERRATUM

Development 136, 507 (2009) doi:10.1242/dev.033530

Evidence for a composite anterior determinant in the hover fly *Episyrphus balteatus* (Syrphidae), a cyclorrhaphan fly with an anterodorsal serosa anlage

Steffen Lemke and Urs Schmidt-Ott

There was an error published in *Development* **136**, 117-127.

In the legend to Fig. 6 on p. 123, the scale bar for M is 222 μm, not 22 μm.

We apologise to authors and readers for this mistake.

Development 136, 117-127 (2009) doi:10.1242/dev.030270

Evidence for a composite anterior determinant in the hover fly *Episyrphus balteatus* (Syrphidae), a cyclorrhaphan fly with an anterodorsal serosa anlage

Steffen Lemke and Urs Schmidt-Ott*

Most insect embryos develop from a monolayer of cells around the yolk, but only part of this blastoderm forms the embryonic rudiment. Another part forms extra-embryonic serosa. Size and position of the serosa anlage vary between species, and previous work raises the issue of whether such differences co-evolve with the mechanisms that establish anteroposterior (AP) polarity of the embryo. AP polarity of the *Drosophila* embryo depends on *bicoid*, which is necessary and sufficient to determine the anterior body plan. Orthologs of *bicoid* have been identified in various cyclorrhaphan flies and their occurrence seems to correlate with a mid-dorsal serosa or amnioserosa anlage. Here, we introduce with *Episyrphus balteatus* (Syrphidae) a cyclorrhaphan model for embryonic AP axis specification that features an anterodorsal serosa anlage. Current phylogenies place *Episyrphus* within the clade that uses *bicoid* mRNA as anterior determinant, but no *bicoid*-like sequence could be identified in this species. Using RNA interference (RNAi) and ectopic mRNA injection, we obtained evidence that pattern formation along the entire AP axis of the *Episyrphus* embryo relies heavily on the precise regulation of *caudal*, and that anterior pattern formation in particular depends on two localized factors rather than one. Early zygotic activation of *orthodenticle* is separated from anterior repression of *caudal*, two distinct functions which in *Drosophila* are performed jointly by *bicoid*, whereas *hunchback* appears to be regulated by both factors. Furthermore, we found that overexpression of *orthodenticle* is sufficient to confine the serosa anlage of *Episyrphus* to dorsal blastoderm. We discuss our findings in a phylogenetic context and propose that *Episyrphus* employs a primitive cyclorrhaphan mechanism of AP axis specification.

KEY WORDS: Fate-map, Developmental constraint, Evolutionary development (EvoDevo), *Bicoid*, *Episyrphus*

INTRODUCTION

The specification of the anteroposterior (AP) axis of the *Drosophila* embryo has been studied in great detail (see Surkova et al., 2008), but the mechanism is not conserved across flies (Diptera). One of the key genes in the *Drosophila* model, *bicoid*, appears to be confined to higher dipterans (Cyclorrhapha) (Lemke et al., 2008; Stauber et al., 2002; Zdobnov et al., 2002). Comparative studies in dipterans are particularly suitable to explore how and why this gene evolved and should lead to a better understanding of factors that shape or constrain mechanisms of AP axis specification in evolution. One suspect is the extra-embryonic serosa anlage, which differs between species in size and position relative to the dimensions of the egg (Roth, 2004). Previous work suggests a correlation between the occurrence of *bicoid* and a mid-dorsal rather than anterior or anterodorsal position of the (amnio-) serosa anlage (Schmidt-Ott, 2005). However, we recently discovered an anterodorsal serosa anlage in the cyclorrhaphan hover fly *Episyrphus balteatus* (Syrphidae) (Fig. 1) (Rafiqi et al., 2008), which seems to contradict this correlation and prompts the question how this species specifies its AP axis.

In *Drosophila*, a long-germ insect with an embryonic rudiment that extends from the anterior to the posterior tip of the egg (Davis and Patel, 2002; Tautz et al., 1994), the amnioserosa anlage is confined to a narrow strip of mid-dorsal blastoderm (Hartenstein, 1993). AP polarity of the *Drosophila* embryo stems in part from symmetrical signaling processes at both poles of the egg, which are mediated by the receptor tyrosine kinase Torso, but is determined by the asymmetric distributions of maternal of *bicoid* and *nanos* mRNAs, which are localized at opposite poles of the egg (reviewed by St Johnston and Nüsslein-Volhard, 1992). The *bicoid* protein is expressed in an anterior-to-posterior gradient and specifies the anterior body plan (Driever and Nüsslein-Volhard, 1988a; Driever and Nüsslein-Volhard, 1988b; Driever et al., 1990). It functions predominantly as a transcription factor and regulates the expression of direct targets such as *orthodenticle* or *hunchback* in a spatially restricted manner (see Berman et al., 2002; Ochoa-Espinosa et al., 2005; Schroeder et al., 2004; Segal et al., 2008). Bicoid activates *orthodenticle* only in a narrow anterior cap but activates *hunchback* throughout the anterior half of the blastoderm (Driever and Nüsslein-Volhard, 1989; Finkelstein and Perrimon, 1990; Gao and Finkelstein, 1998; Gao et al., 1996; Struhl et al., 1989). In addition to its role as a transcriptional regulator, Bicoid directly represses the translation of ubiquitous maternal *caudal* transcripts (see Cho et al., 2005), which would otherwise interfere with proper head development (Mlodzik et al., 1990; Niessing et al., 1999). The *nanos* protein is expressed in a posterior-to-anterior gradient and is essential to suppress the posterior translation of ubiquitous maternal *hunchback* transcripts, which would interfere with abdominal patterning (Tautz, 1988). This process is mediated by Nanos-response-elements (NREs) in the 3′ untranslated region (UTR) of *hunchback* mRNA (Murata and Wharton, 1995; Sonoda and Wharton, 1999; Sonoda and Wharton, 2001) (reviewed by Vardy and Orr-Weaver, 2007; Wharton and Struhl, 1991). As Nanos is not crucially required in other segmentation mechanisms (Hülskamp et al., 1989; Irish et al., 1989; Struhl, 1989), *bicoid* is the only essential

University of Chicago, Department of Organismal Biology and Anatomy, CLSC 921B, 920 E. 58th Street, Chicago, IL 60637, USA.

*Author for correspondence (e-mail: uschmid@uchicago.edu)

Accepted 23 October 2008

determinant of AP polarity in the *Drosophila* embryo. In many other cyclorrhaphan flies, this fundamental role of *bicoid* is probably conserved, because in *Megaselia*, a basal cyclorrhaphan taxon, suppression of *bicoid* results in a mirror image duplication of the posterior abdomen, i.e. the loss of global AP polarity (Lemke et al., 2008; Stauber et al., 2000).

Alternative models for specifying AP polarity of insect embryos have been proposed for *Nasonia* (a wasp) and *Tribolium* (a beetle). For *Tribolium*, a short-germ insect with a large anterior serosa anlage (Falciani et al., 1996), it has been proposed that *orthodenticle* (*Tc-otd1*) and *hunchback* (*Tc-hb*) substitute for *bicoid* (Schröder, 2003). The ubiquitous maternal mRNAs of both genes contain potential NRE sequences that might explain their posterior repression, although at first both mRNAs are translated throughout the blastoderm (Schröder, 2003; Wolff et al., 1995). *Tc-otd1* and *Tc-hb* function in a synergistic manner and control the formation of all but two abdominal segments. All postoral segments also require *Tribolium caudal* (*Tc-cad*), another maternally expressed gene that is initially translated throughout the blastoderm but then repressed anteriorly (Copf et al., 2004; Schulz et al., 1998). Thus, although the initial symmetry-breaking factors along the AP axis of the *Tribolium* egg remain poorly characterized, AP polarity of the *Tribolium* embryo can be explained by three maternal gradients.

Nasonia evolved long-germ development independently of *Drosophila* and develops likewise a dorsal serosa anlage that, unlike in *Drosophila*, reaches almost to the anterior tip of the embryo (Pultz et al., 2005). This species localizes maternal transcripts of *giant* (*Nvit gt*) at the anterior pole (Brent et al., 2007) and of *caudal* (*Nvit cad*) at the posterior pole (Olesnicky et al., 2006). In addition, *Nasonia* embryos localize maternal transcripts of *orthodenticle* (*Nvit otd1*) at the anterior and the posterior pole (where translation is delayed) (Lynch et al., 2006). *Nvit otd1* and *Nvit gt* are required for head development, but *Nvit gt* has only a permissive role because the loss-of-function phenotype caused by *Nvit gt* RNA interference (RNAi) is rescued by double RNAi against *Nvit gt* and the head repressor *Nvit Kr*, a homolog of *Krüppel* (Brent et al., 2007). Unlike *bicoid* in *Drosophila*, *Nvit otd1* has only a modest effect on anterior *hunchback* (*Nvit hb*) expression, but like *bicoid*, *Nvit otd1* functions in synergism with anterior *Nvit hb* in specifying head, thorax, and anterior abdomen (Lynch et al., 2006). *Nvit cad* is required for thorax and abdomen development (Olesnicky et al., 2006; Pultz et al., 1999). Finally, because of NRE-like sequences in the mRNAs of *Nvit otd1* and *Nvit hb*, it has been suggested that AP polarity of the *Nasonia* embryo also depends on a homolog of *nanos* (Lynch et al., 2006).

In this article, we take advantage of the experimental amenability of *Episyrphus* to explore AP axis specification in a close relative of *Drosophila* and *Megaselia* that specifies an anterodorsal rather than a mid-dorsal (amnio-) serosa anlage and develop a new model for early AP axis specification in cyclorrhaphan flies.

MATERIALS AND METHODS

Episyrphus culture

Episyrphus balteatus Degeer (Diptera: Syrphidae) was reared as populations of 300-600 adult flies in cages (45×65×90 cm^3) made of mosquito netting. Adult flies were fed on honey and ground bee pollen. For egg deposition, 7-14 day old adults were provided with *Vicia faba* seedlings (15-20 cm), infested with the green pea aphid (*Acyrthosiphon pisum*). New generations were set up by feeding larvae on green pea aphids for 9-11 days until pupation, and adults eclosed 5-6 days after pupation. The overall generation time at 25°C, a 14/10 hours light/dark cycle (light intensity: 4000 Lux) and a~50% relative humidity was 24-26 days.

Cloning procedures

Fragments of *Episyrphus* homologs have been obtained by PCR using degenerate primers for *hunchback* (Stauber et al., 2000), *nanos* (5′-TGYGTGTTYTGYRARAAYAA/5′-GGYTTYTTNGGRCARTAYTT), *caudal* (Stauber et al., 2008) and *orthodenticle* (5′-GGRTTYYCNC-AAGGTATGTGGG/5′-ACCTGWACTCKWGATTCNGG). A fragment of the *Eba-otd* homeodomain was also obtained with degenerate *bicoid* primers (5′-TNGTNATGMGNMGNMGNMGNAC/5′-CKNCKRTTYT-TRAACCA). cDNA was prepared from poly(A^+) RNA of 0 to 5-hour-old embryos (collected at 25°C) using the SMART RACE cDNA Amplification Kit (Clontech). In the case of *Eba-hb*, we isolated three transcripts with a common open reading frame and alternative first exons in the 5′ UTR (see Table S1 in the supplementary material) (S. Lemke, 2006, PhD thesis, Molecular Biology Program, Georg-August-Universität, Göttingen). Double-stranded RNA was generated from nucleotides 198 to 1033 of the *Eba-hb* open reading frame (ORF), nucleotides 65 to 671 of the *Eba-nos* ORF, 162 nucleotides of the 5′ UTR and adjacent nucleotides 1 to 686 of the *Eba-cad* ORF, and nucleotides 250 to 987 of the *Eba-otd* ORF plus adjacent 67 nucleotides of 3′ UTR. To create the template for capped *Eba-nos* mRNA, cDNA was PCR amplified with the primer pair 5′-CATGCC-ATGGGTTATCCTGACGACATGTATAGAAATAAC/5′-ACGCGTCGA-CTTAAGCCTTCATGTGGTGCTTGAAATAGCT, digested with *Nco*I and *Sal*I, and cloned into pSP35 (Amaya et al., 1991). The template for capped *Eba-otd* mRNA was created accordingly using the primer pair 5′-CATGCCATGGCAGCGGGCTTTTTAAAATCTGGTGAT/5′-ACGCGT-CGACTACACCATATTCACATACTTGTCTTGG. An *Nco*I site within the *Eba-cad* ORF was deleted by generating two overlapping PCR fragments with the primer pairs 5′-CATGCCATGGTTTCCTATTATAACTCT-CTCTCATAT/5′-GGTAATTCGATTGCCATGCCCAGGGTTGAC and 5′-GTCAACCCTGGGCATGGCAATCGAATTACC/5′-ACGCGTCGACT-CACATTGACAGCGCACCTACAGAGGCGGC, and reconstituting the full ORF from the two fragments using only terminal primers. The product was digested with *Nco*I and *Sal*I, and cloned into pSP35. To synthesize capped mRNA with the 5′ and 3′ flanking sequences of *Xenopus*-globin, plasmids were linearized with *Eco*RI (*Eba-nos*, *Eba-cad*) or *Pst*I (*Eba-otd*), and transcribed using the SP6 mMessage mMachine Kit (Ambion). Embryos were injected as described (Rafiqi et al., 2008).

In situ hybridization, antibody staining, and cuticle preparation

RNA probes for histochemical detection were all labeled with digoxigenin as we experienced background problems in pre-syncytial blastoderm embryos with fluorescein- and biotin-labeled probes. For fluorescent detection at later stages, the probes were labeled with fluorescein (*Eba-hb*) and biotin (*Eba-zen*). Embryo fixation and in situ hybridization were performed essentially as described (Kosman et al., 2004; Tautz and Pfeifle, 1989). The *Eba-hb* probe comprised 163 nucleotides of 5′ UTR and adjacent nucleotides 1 to 889 of the ORF, the *Eba-nos* probe comprised 174 nucleotides of 5′ UTR and adjacent nucleotides 1 to 544 of the ORF, the *Eba-cad* probe comprised nucleotides 94 to 1032 of the ORF, and the *Eba-otd* probe comprised nucleotides 218 to 987 and adjacent 114 nucleotides of 3′ UTR. Engrailed was detected using the cross-specific monoclonal antibody 4D9 (1/10 dilution) (Patel et al., 1989) as primary antibody, a biotinylated horse anti-mouse (1/500 dilution; Vector Laboratories) as secondary antibody, and alkaline phosphatase-conjugated anti-biotin FAB-fragments (1/2000 dilution; Roche) as tertiary antibody. Staining was carried out as described (Schmidt-Ott and Technau, 1992) with the following modifications: embryos were fixed in a 1:1 mixture of n-heptane and 3.7% formaldehyde in PEM (0.1 M PIPES, 2 mM $MgSO_4$, 1 mM EGTA, pH 6.9) for 60 minutes on a shaker. Injected embryos were postfixed for 30 minutes in 3.7% formaldehyde in PBT (0.13 M NaCl, 7 mM Na_2HPO_4, 3 mM NaH_2PO_4, 0.1% Tween-20) after devitellinization. Incubation with the secondary antibody was carried out for 2 hours, incubation with the tertiary antibody for 1 hour at room temperature. Embryos were stained in AP (0.1 mM NaCl, 0.05 M MgCl, 0.1 M Tris pH 9.5, 0.1% Tween-20) with NBT (0.08 μg/μl)/BCIP (0.04 μg/μl) overnight at 4°C. *Episyrphus* first instar cuticles were mounted as described (Stern and Sucena, 2000) with a 2:1 mixture of Hoyer's medium and lactic acid.

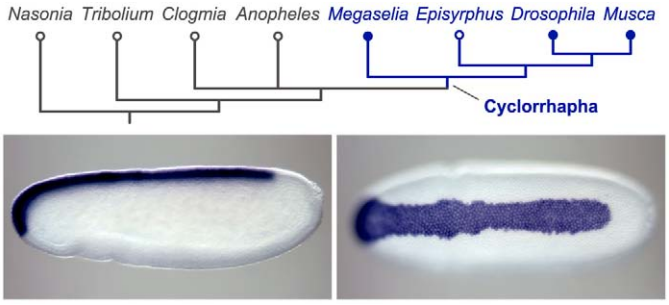

Fig. 1. Phylogenetic occurrence of *bicoid* and anterodorsal serosa anlage of *Episyrphus*. Taxa with *bicoid* are marked by a filled circle. The serosa anlage was labeled by in situ hybridization using an *Eba-zen* probe. The same embryo is shown in lateral (left) and dorsal (right) views with the anterior towards the left.

RESULTS

Segmental markers in wildtype embryos and the first instar cuticle of *Episyrphus*

A comprehensive description of embryonic development in *Episyrphus* or any other hover fly is currently not available. In this section, we therefore provide a description of the markers in the wild-type embryo that we used to characterize specific phenotypes. Embryonic development of *Episyrphus* lasts about 2 days at 25°C. The syncytial blastoderm forms after 3 hours and cellularization of the blastoderm begins at 4 hours of development. Previously, we have shown that *Episyrphus* expresses homologs of the pair-rule genes *even skipped* (*Eba-eve*) and *hairy* (*Eba-h*) prior to gastrulation in seven stripes, indicating that it is a long-germ insect like other cyclorrhaphan flies (Bullock et al., 2004). To determine the developmental stage at which *Eba-eve* and *Eba-h* can be used as segmentation markers, we followed the expression of these genes in early embryos. Prior to the onset of cellularization, the expression of both genes appeared dynamic (see Fig. S1 in the supplementary material). The seven *Eba-eve* stripes of later blastoderm stages and gastrulating embryos were complemented by weaker *Eba-eve* inter-stripes, and all *Eba-eve* stripes were repressed along the dorsal midline (Fig. 2A-B′). The seven transverse *Eba-h* stripes were also repressed along the dorsal midline but most of the serosa anlage of older blastoderm embryos expressed *Eba-h* (Fig. 2C-D′). An eighth *Eba-h* stripe at the posterior end of gastrulating embryos retained its dorsal continuity (Fig. 2D,D′).

To distinguish segments in the embryonic germband, we used a cross-reacting antibody against Engrailed (Patel et al., 1989). This antibody allowed us to distinguish the ocular, antennal, intercalary, mandibular, maxillar and labial segments of the head, the three thoracic segments (T1-3) and nine abdominal segments (A1-9) (Fig. 2E-F′). In the clypeolabrum, Engrailed was expressed in a (weak) patch (Fig. 2F), and in the hindgut Engrailed was expressed in a narrow circular ring (not shown).

Denticles of first instar cuticles provided unique markers for each of the three thoracic segments T1, T2 and T3, the first abdominal segment A1, abdominal segments A2-7 and abdominal segment A8 (Fig. 3A-C). The most posterior cuticle markers were a pair of ‘Filzkörper’. These structures line the inner wall of the posterior spiracles and are probably an A8 derivative. The cephalopharyngeal skeleton, and the ‘antennomaxillary complex’ (including the antenna and the maxillary sense organ) provided cuticular markers for the head region. Within the cephalopharyngeal skeleton we distinguished an anterior ‘median tooth’ (presumably a clypeolabral derivative), a pair of mouth-hooks, a medioventral ‘H-piece’, as well as bilateral ‘cephalopharyngeal plates’, ‘neck clasps’ and ‘Lateralgräten’ (Fig. 3D-H).

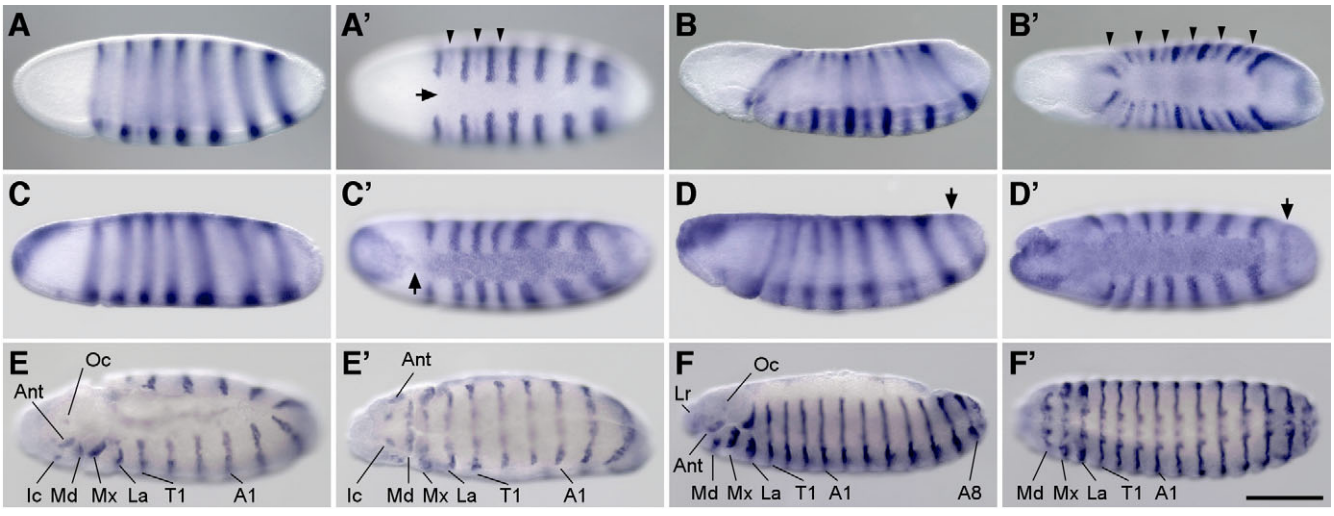

Fig. 2. Expression of *Eba-eve*, *Eba-h* mRNA and Engrailed in *Episyrphus*. (**A-B’**) *Eba-eve* expression at (A,A′) and shortly after (B,B′) the beginning of gastrulation. Note the clearance of *Eba-eve* expression along the dorsal midline (arrow in A′) and the interstripes (arrowheads in A′ and B′). (**C-D’**) *Eba-h* expression at (C,C′) and shortly after (D,D′) the beginning of gastrulation. Note the gap in *Eba-h* expression in the serosa anlage (arrow in C′) and in the eighth stripe (arrows in D,D′). (**E-F’**) Engrailed pattern in *Episyrphus* embryos as detected by 4D9 antibody at the extended germband stage (E,E′) and after germband retraction (F,F′). Expression in the clypeolabrum (Lr), the ocular segment (Oc), the antennal segment (Ant), the intercalary segment (Ic), the mandibular segment (Md), the maxillar segment (Mx), the labial segment (La), T1, A1 and A8 is indicated. Each embryo is shown with anterior towards the left in lateral (A-F) and dorsal (A′-D′) or ventral (E′-F′) view. Scale bar in F′: 200 μm for A,A′,C-E′; 240 μm for B,B′; 190 μm for F,F′.

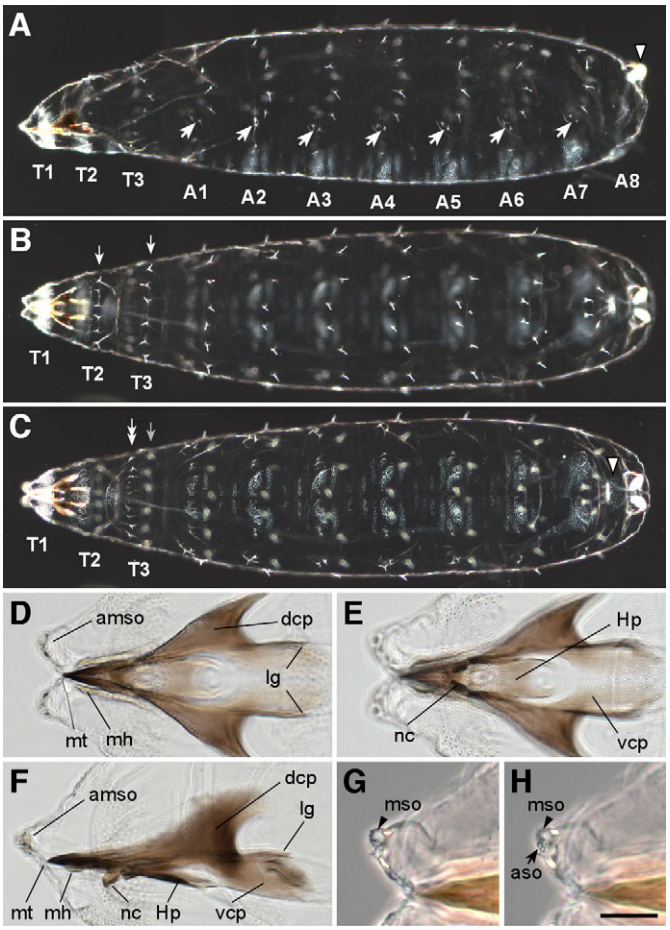

Fig. 3. Cuticle of the first-instar larva. (**A-C**) Cuticles in lateral (A), dorsal (B) and ventral (C) view in dark-field optics. Filzkörper (fk) within the posterior spiracles (arrowhead in A), and the reduced denticle field of A8 (arrowhead in C) posterior of the presumptive anal slit are indicated. Lateral denticle doublets (arrows in A), which are characteristic for abdominal segments A1 to A7, are present. Thoracic segments T2 and T3 (arrows in B) and abdominal segments A1 to A7 share a single row of large dorsal denticles. T3 has a unique row of large ventral denticles (double arrow in C; the dorsal denticle row, which is out of focus, is marked by a gray arrow). (**D-H**) Magnified dorsal (D,E,G,H) and lateral (F) views of the antennomaxillary complex (amso) and cephalopharyngeal skeleton in phase contrast. The antennomaxillary complex includes the maxillary (mso) and the antennal sense organ (aso). The cephalopharyngeal skeleton includes a median tooth (mt), mouth hooks (mh), dorsal and ventral cephalopharyngeal plates (dcp, vcp), H-piece (Hp), neck clasps (nc), and Lateralgräten (lg). Anterior is towards the left. Scale bar in H: 180 μm for A; 200 μm for B,C; 44 μm for D-F; 27 μm for G,H.

Expression of *hunchback*, *nanos*, *caudal* and *orthodenticle* homologs in *Episyrphus*

Current phylogenies place *Episyrphus* close to the monophyletic higher Cyclorrhapha (Schizophora) (Grimaldi and Engel, 2005; Yeates and Wiegmann, 2005), i.e. within the clade that uses *bicoid* mRNA as anterior determinant (Fig. 1; see Fig. S2 in the supplementary material) but we have not been able to identify any *bicoid*-like gene in this species. We performed PCR on cDNA and genomic DNA templates of *Episyrphus* using various sets of degenerate PCR primers spanning conserved regions of *bicoid* inside and outside the homeobox. These experiments yielded homeobox fragments that were homologous to *zerknüllt* (Rafiqi et al., 2008) and *orthodenticle* (Michael Stauber and U.S.-O., unpublished). Because of the conserved genomic position of *bicoid* immediately upstream of its paralogous sister gene *zerknüllt* (Brown et al., 2001; Negre et al., 2005), we also sequenced ~79 kb of the *Episyrphus zerknüllt* (*Eba-zen*) locus, including ~60 kb upstream of this gene but this approach did not yield a *bicoid*-like sequence either (A. M. Rafiqi, J. Raedts, O. Schön, H. Blöcker and U.S.-O., unpublished).

To begin exploring the sources of AP polarity in the *Episyrphus* embryo without an apparent *bicoid* homolog, we isolated homologs of *hunchback* (*Eba-hb*), *nanos* (*Eba-nos*), *caudal* (*Eba-cad*) and *orthodenticle* (*Eba-otd*) (see Fig. S3 in the supplementary material) and studied their expression by in situ hybridization of whole-mount ovarian follicles and embryos. *Episyrphus* embryos seem to lack significant maternal *Eba-hb* mRNA because neither ovarian follicles (see Fig. S4A,B in the supplementary material) nor pre-blastoderm embryos were stained with an *Eba-hb* probe (see also note in Materials and methods). Zygotic expression was first detected during the early syncytial blastoderm stage and extended from 0% (anterior pole) to 90% egg-length (EL) with a fuzzy posterior boundary (Fig. 4A). This pattern indicates that initial *Eba-hb* expression is under the control of one or more factors with an almost ubiquitous distribution. One nuclear division cycle later, *Eba-hb* expression had strongly increased, and the still fuzzy posterior boundary had shifted anteriorly to ~75% EL (Fig. 4B). At the onset of cellularization, the posterior boundary had sharpened and was positioned at about 50% EL. Older blastoderm embryos also expressed *Eba-hb* at the posterior pole (Fig. 4C) and along the dorsal midline (Fig. 4D-F). At the onset of gastrulation, the dorsal domain coincided exactly with the serosa anlage (see Fig. S4C-E′ in the supplementary material) but in slightly older embryos this domain appeared to be centered on the boundary region between prospective serosa and amnion (Fig. 4G). *Eba-hb* was also expressed in the central nervous system and in yolk nuclei (Fig. 4H).

Eba-nos transcripts were detected throughout early embryos and were enriched in the posterior pole plasm (Fig. 4I). Somatic transcripts disappeared during cellularization but the germ cells continued to express *Eba-nos* in older embryos (Fig. 4J-L).

Eba-cad mRNA was detected in the nurse cells and the oocyte and of ovarian follicles (see Fig. S4B in the supplementary material) and was evenly distributed in early embryos (Fig. 4M). At the syncytial blastoderm stage, the anterior embryo (0%-20% EL) was cleared of *Eba-cad* transcripts, whereas strong zygotic expression was observed in the remaining blastoderm except in the pole cells (Fig. 4N,O). In subsequent blastoderm stages, *Eba-cad* expression was gradually reduced to a posterior ring, which persisted through gastrulation as a ring closing about the proctodeum (Fig. 4P-R). Other tissues did not express *Eba-cad* until germband retraction, at which stage a new expression domain was visible in the posterior midgut (Fig. 4S,S′).

Eba-otd mRNA was not detected until the onset of blastoderm cellularization. At this stage, *Eba-otd* was expressed in a cap spanning the anterior pole (Fig. 4T). Slightly older embryos expressed *Eba-otd* in two lateral anterior patches but not along the dorsal midline (Fig. 4U-V′). During germband extension, *Eba-otd* was also expressed along the ventral midline and in segmental neuroblasts of the gnathocephalic, thoracic and abdominal segments (Fig. 4W-X′).

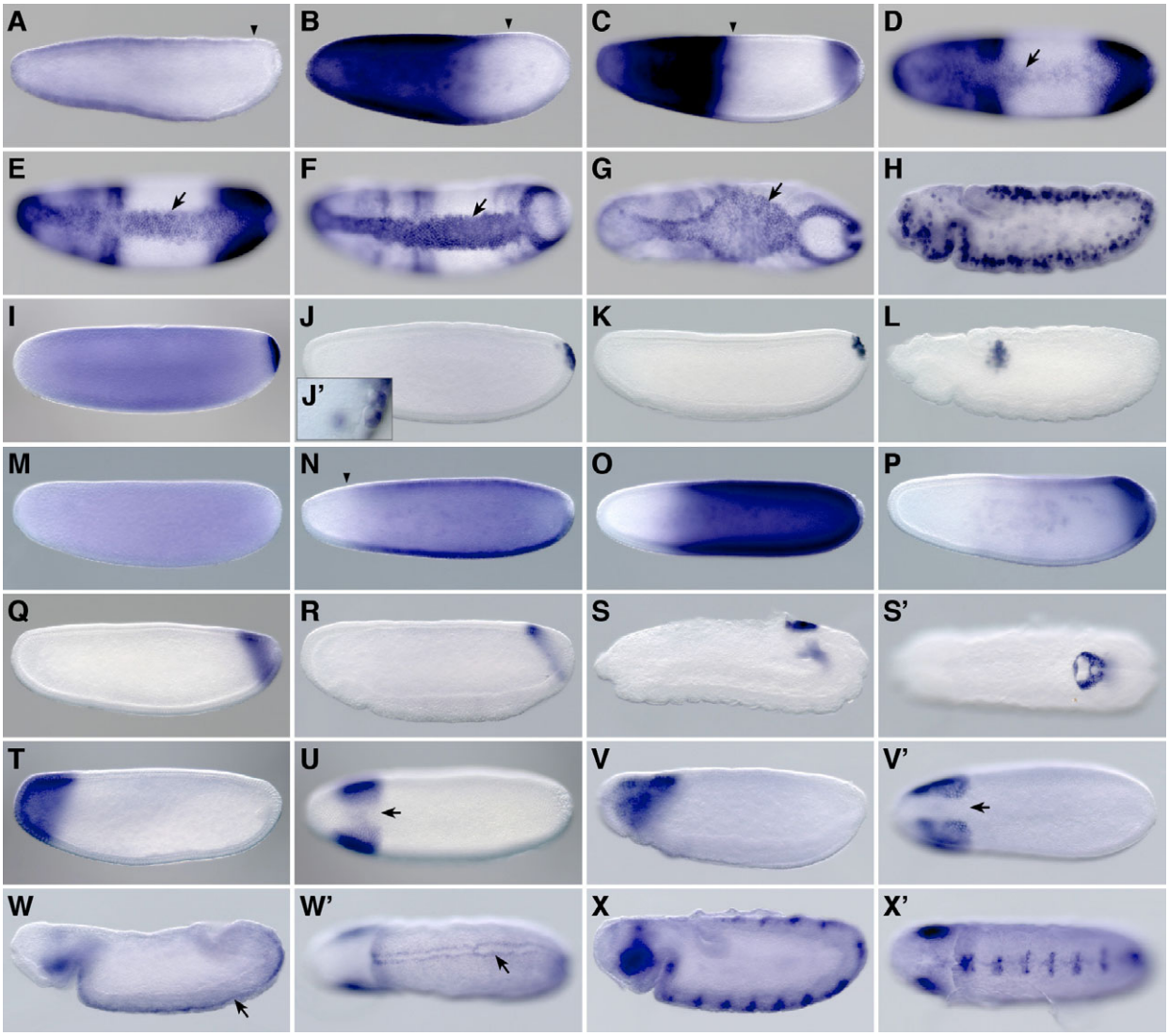

Fig. 4. Expression of *Eba-hb*, *Eba-nos*, *Eba-cad* and *Eba-otd* mRNA. (**A-H**) *Eba-hb* expression during subsequent blastoderm (A-F) and gastrulation stages (G-H). Note the posterior boundary of the anterior domain (arrowheads in A-C) and extra-embryonic expression (arrows in D-G). (**I-L**) *Eba-nos* expression before (I), at the beginning of (J) and during (K) cellularization, as well as in the extended germband (L). Within pole cells, the transcripts were predominantly localized in the posterior half (J'). (**M-S'**) *Eba-cad* expression before blastoderm formation (M), during consecutive blastoderm stages (N-Q), at the beginning of gastrulation (R) and during germband retraction (S,S'). Note the anterior boundary of the early zygotic expression domain (triangle in N). (**T-X'**) *Eba-otd* expression at the onset of cellularization (T), during cellularization (U), at the onset of gastrulation (V,V') and during germband extension (W-X'). Note clearance along the dorsal midline of the blastoderm (arrows in U,V'), and expression along the ventral midline (arrows in W,W') and in the developing nervous system (X,X'). Embryos are shown with anterior towards the left in lateral view, except in D-G,J',S',V' and W',X', which are dorsal and ventral views, respectively.

Anterior pattern formation depends on two distinct localized factors that function upstream of *Eba-hb*, *Eba-otd* and *Eba-cad*

The posteriorly enriched maternal mRNA of *Eba-nos* raises the issue of whether this gene serves as a determinant of AP polarity in the *Episyrphus* embryo. Furthermore, putative NREs in the 3′ UTRs of *Eba-hb* and *Eba-otd* (Fig. 5A) raise the issue of whether the Nanos-dependent regulation of *Eba-hb* and *Eba-otd* is important for embryonic development despite the absence of maternal transcripts of these genes in early embryos. To address these issues we induced *Eba-nos* RNAi in very early embryos but these experiments did not perturb the process of segmentation. Resulting cuticles were indistinguishable from wild type (n=63; data not shown) and the majority of the larvae hatched, even when double-stranded RNA was injected within the first 15 minutes of development, i.e. prior to the first nuclear division cycle. We verified efficient degradation of *Eba-nos* transcripts following RNAi by in situ hybridization with an *Eba-nos* probe and detected *Eba-nos* transcripts in only one of 48 embryos. These results suggest that *Eba-nos* mRNA in the embryo is not essential for segmentation.

To test whether *Eba-nos* stabilizes AP polarity by repressing anterior development, we injected capped *Eba-nos* mRNA at various positions of the embryo and examined the gain-of-function phenotypes in cuticles. Anterior injection of *Eba-nos* mRNA

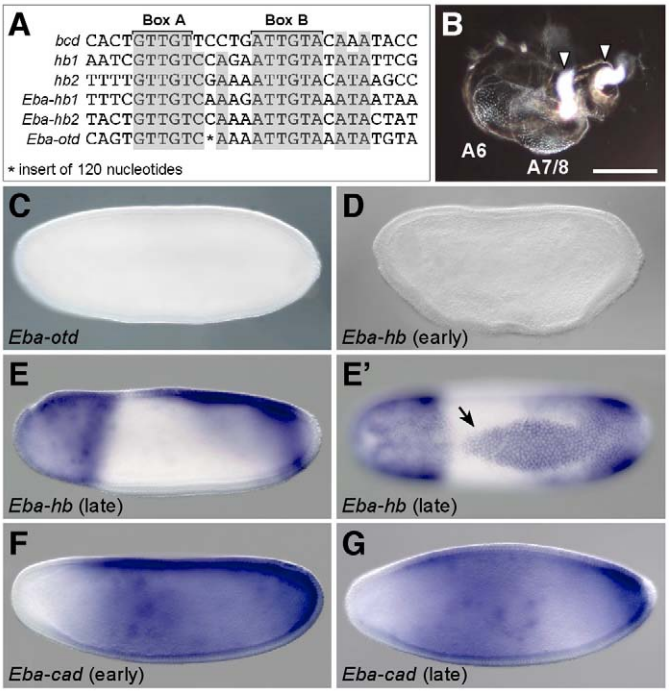

Fig. 5. Ectopic *Eba-nos* activity suppresses anterior development. (**A**) Comparison of *bicoid* (*bcd*) and *hunchback* (*hb*) NREs with NRE-like sequences in the 3′UTRs of *Eba-hb* and *Eba-otd*. (**B-G**) Phenotypes caused by double-injection of *Eba-nos* mRNA at the anterior pole (0% EL) and ~25% EL. Note the complete absence of anterior cuticular markers (B; triangles mark the Filzkörper). Note also the absence of *Eba-otd* expression during blastoderm cellularization (C) and *Eba-hb* expression prior to (D) but not shortly after (E,E′) the onset of cellularization, when expression resumes in an anterior cap. Extra-embryonic *Eba-hb* expression (arrow in E′) is confined to mid-dorsal blastoderm. Early *Eba-cad* expression (F) is not affected, but *Eba-cad* transcript degradation in older blastoderm embryos is perturbed (G). Anterior is towards the left. Embryos are shown in lateral (C-G) or dorsal (E′) view. Scale bar in B: 200 μm.

disrupted segmentation in the head, thorax and anterior abdomen. When *Eba-nos* mRNA was injected at the anterior tip, 67% of the cuticles lacked head elements, 35% exhibited missing head and thorax markers and 14% lacked most of the anterior body, including A1 and A2 (*n*=66) (see Fig. S5A in the supplementary material). In a single cuticle the head, the thorax and abdominal segments A1-A5 were missing. When *Eba-nos* mRNA was injected twice, once at the anterior tip and once at about 25% EL (but in reduced quantity so as to roughly match the amount of injected mRNA with single injections in the previous experiment), the resulting cuticles exhibited on average much stronger phenotypes with deletions in the head, thorax and abdomen (72%, *n*=18) (see Fig. S5B in the supplementary material), but the strongest phenotype (head, thorax and A1-A5 missing) of cuticles from double-injected embryos was identical to the strongest phenotype of cuticles from single-injected embryos (Fig. 5B). These results show that ectopic *Eba-nos* interferes effectively with anterior development.

To explore the genetic causes of this phenotype, we analyzed *Eba-otd*, *Eba-hb* and *Eba-cad* expression at the blastoderm stage of embryos that had been double-injected with *Eba-nos* mRNA. *Eba-otd* expression was reduced (29%; *n*=24) or absent (33%) (Fig. 5C). For *Eba-hb* and *Eba-cad*, we noticed stage-specific effects. Prior to the onset of cellularization, *Eba-hb* expression was absent (15%; *n*=13) (Fig. 5D) or the posterior boundary of the anterior *Eba-hb* domain was shifted towards the anterior pole by 10-20% (69%). In embryos that had started to cellularize, the anterior *Eba-hb* domain was never fully suppressed but its posterior boundary was shifted towards the anterior pole by 10-20% compared with wild-type embryos of the same stage (75%; *n*=20) (Fig. 5E,E′). These results suggest that anterior *Eba-hb* expression is controlled by more than one factor. Early *Eba-cad* expression was not affected (*n*=12) (Fig. 5F). Only during blastoderm cellularization did a fraction of the embryos express *Eba-cad* ectopically, though not at the anterior pole (44%, *n*=9) (Fig. 5G). Hence, the anterior repression of *Eba-cad* transcripts is independent of the factors regulated by ectopic *Eba-nos*.

To determine whether ectopic *Eba-nos* causes abdominal phenotypes due to interference with a factor that is produced in the anterior or the posterior embryo, we also examined cuticles from embryos that had been injected with *Eba-nos* mRNA at the posterior pole. These cuticles were mostly indistinguishable from wild type (70%, *n*=87) and many of the larvae hatched. Some cuticles exhibited defects in T3 and/or A1 (24%), which might best be explained by translational repression of *Eba-hb* (see below). In other parts of the embryo, suppression of markers was observed only sporadically (6%) (see Fig. S5C in the supplementary material). In particular, posterior *Eba-nos* mRNA injection caused defects posterior to A1 much less frequently than anterior *Eba-nos* mRNA injection. As a negative control we injected dsRed mRNA at the anterior or the posterior pole. These embryos developed a cuticle that was indistinguishable from wild type and mostly hatched. Together, these results suggest that ectopic *Eba-nos* activity targets mRNA that is localized to the anterior embryo.

To test whether the maximal *Eba-nos* gain-of-function phenotype can be explained by Nanos-dependent translational repression of *Eba-otd* and *Eba-hb*, we compared this phenotype with the RNAi phenotypes of *Eba-hb* and *Eba-otd*. *Eba-hb* RNAi cuticles exhibited wild-type denticles in abdominal segments A2-6 (100%, *n*=37) (Fig. 6A). T1-T3 denticles were absent, and A1 denticles were reduced (25%) or absent (75%). The denticle fields of A7 and A8 were reduced, and could not be distinguished from each other, whereas the Filzkörper were lost or reduced and spread apart. The median tooth was arc shaped, presumably because the clypeolabrum failed to involute, and the cephalopharyngeal skeleton appeared shortened and reduced (Fig. 6B). In particular, the H-piece was missing. However, the antennae, maxillary sense organs, mouth hooks and neck clasps were present (Fig. 6C,D). *Eba-hb* RNAi embryos lacked Engrailed expression in the labial and thoracic segments, and in the A1 epidermis (except for an Engrailed expressing cell in the anterior dorsal compartment that is characteristic for abdominal segments A1-7) (Fig. 6E,E′).

In *Eba-otd* RNAi cuticles, the cephalopharyngeal skeleton was strongly reduced and the antennae were missing but the mouth hooks, neck clasps and maxillary sense organs were present (Fig. 6F-I). In addition, the ventral denticle fields were interrupted along the midline (compare Fig. 3C with Fig. 6F). In strong RNAi phenotypes, all thoracic and abdominal segments exhibited this defect. Less severe phenotypes showed this defects only in segments posterior to T1 or T2. In about 50% of the specimens, we noticed a cuticular irregularity between the ventral denticle fields of A4 and A5. *Eba-otd* RNAi embryos consistently lacked Engrailed markers of the ocular and antennal segments (Fig. 6J-K). The intercalary segment and the clypeolabrum were shifted anterodorsally and the stomodeum opened to the dorsal side (Fig. 6J′).

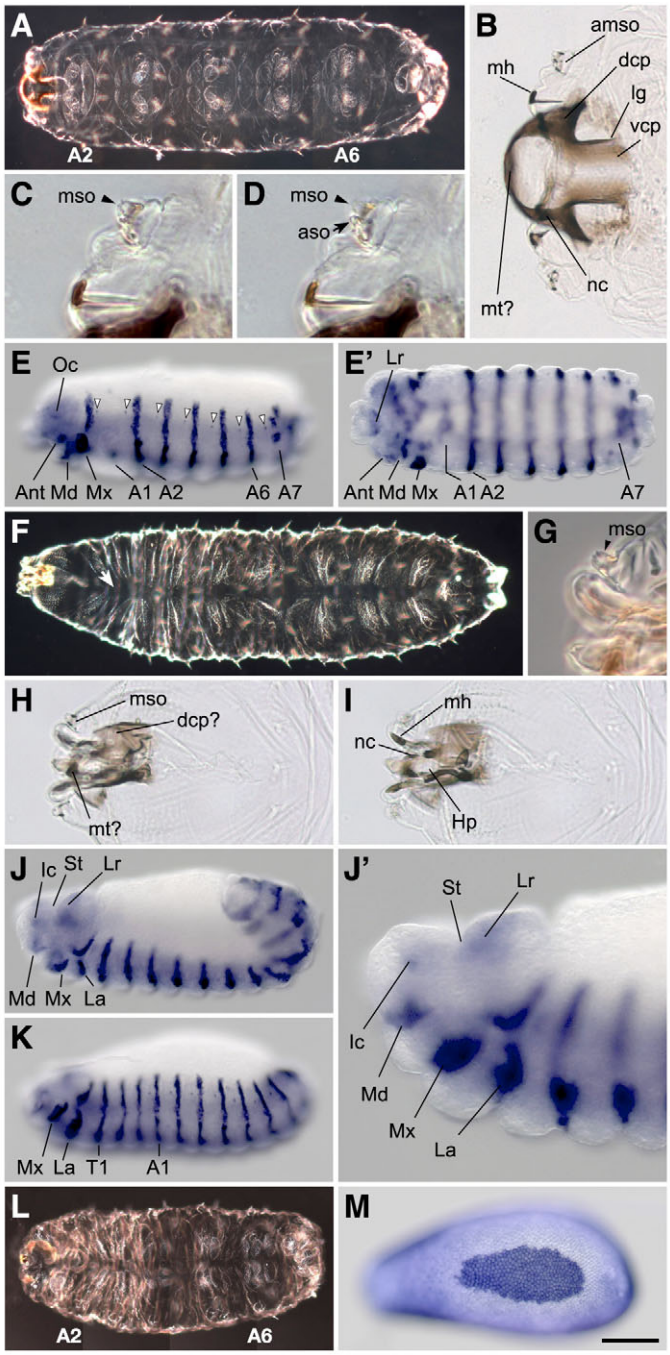

Fig. 6. Functional analysis of *Eba-hb* and *Eba-otd*. (**A-E'**) *Eba-hb* RNAi phenotype. Overview of the cuticular phenotype in ventral view (A), details of the head cuticle in dorsal view (B-D) and Engrailed expression after germband retraction in lateral (E) and ventral view (E'). Note that A1 retains the Engrailed-positive cell in the anterior compartment, which is characteristic for segments A1 to A7 (arrowheads in E). (**F-K**) *Eba-otd* RNAi phenotype. Overview of the cuticular phenotype in ventral view (F), details of the head cuticle in dorsal view (G-I), and Engrailed expression during (J,J') and after (K) germband retraction in dorsolateral (J) and lateral (J',K) view. Note the dorsal position of the stomodeum (St). (**L**) Double RNAi against *Eba-hb* and *Eba-otd*. The cuticular phenotype, shown here in ventral view, is essentially additive. (**M**) Ectopic anterior *Eba-otd* activity represses anterior expression of *Eba-zen*. The embryo (dorsal view) had been injected with *Eba-otd* mRNA at 0% EL and was stained after attaining the cellular blastoderm stage with an in situ probe against *Eba-zen*. In all panels anterior is towards the left. Ant, antennal segment; amso, antennomaxillary complex; aso, antennal sense organ; dcp, dorsal cephalopharyngeal plate; Hp, H-piece; La, labial segment; Lr, clypeolabrum; lc, intercalary segment; lg, Lateralgräten; Md, mandibular segment; Mx, maxillar segment; mh, mouth hooks; mso, maxillary sense organ; mt, median tooth; nc, neck clasps; Oc, ocular segment; vcp, ventral cephalopharyngeal plate. Scale bar in M: 200 μm for A,E,E'; 73 μm for B; 36 μm for C,D; 342 μm for F; 57 μm for G; 117 μm for H,I; 186 μm for J; 82 μm for J'; 211 μm for K; 285 μm for L; 22 μm for M.

Double RNAi against *Eba-hb* and *Eba-otd* resulted in cuticles with an additive phenotype. All segments posterior to A1 could be identified in all but one cuticle (98%), and an arc-shaped median tooth could be unambiguously identified in 38% of the cuticles (n=64) (Fig. 6L). A single cuticle lacked segmentation and displayed a strongly reduced cephalopharyngeal skeleton. In summary, ectopic anterior *Eba-nos* expression causes a much stronger phenotype than the combined loss of *Eba-otd* and *Eba-hb* activities, and must therefore repress the activity of at least one additional gene (Factor 1). Repression of this factor, however, does not lead to anterior *caudal* expression, and is not sufficient to suppress *hunchback* expression in a narrow anterior cap, suggesting the presence of a second anterior factor that does not respond to ectopic *Eba-nos* (Factor 2). Thus, our gain-of-function experiments with *Eba-nos* suggest that anterior pattern formation in *Episyrphus* is controlled by two independent anterior factors.

Repression of *Eba-otd* allows anterior serosa specification

As shown above, *Eba-otd* activation in the anterior blastoderm depends on a Nanos-responsive factor. However, the effect of this factor on anterior *Eba-otd* expression is overridden by serosa patterning (Fig. 4U), indicating that *Eba-otd* specifically promotes head development. *Eba-otd* RNAi had no obvious effect on the expression of *Eba-cad* (n=47) or *Eba-hb* (n=42), and neither *Eba-hb* RNAi (n=19) nor *Eba-cad* RNAi (n=37) had any obvious effect on blastoderm expression of *Eba-otd* (data not shown). When *Eba-otd* mRNA was injected at the anterior pole anterior serosa, specification through *Eba-zen* was repressed. In 97% (n=36) of these embryos, the serosa anlage was confined to dorsal blastoderm (Fig. 6M). Thus, anterior serosa specification depends on the regulation of *Eba-otd*.

Precise regulation of *Eba-cad* is required for embryonic development and segmentation

Eba-cad RNAi embryos rarely survived until the cuticle stage. The few cuticles that we obtained exhibited a strongly reduced cephalopharyngeal skeleton, a single field of small denticles similar to those in T1 or T2, and sclerotized material at the posterior end (n=6) (Fig. 7A). The presumptive median tooth was arc shaped. Mouthhooks, neck clasps and the antennomaxillary complex were tentatively identified (Fig. 7B-D). Engrailed expression of RNAi embryos was strongly reduced and restricted to the head region (Fig. 7E-F'). The expression of pair-rule genes was reduced to one (*Eba-eve*) (Fig. 7G) or two anterior stripes (*Eba-h*) (Fig. 7H). The *Eba-h* stripes appeared dorsally incomplete and all stripes were shifted towards the posterior pole by about 5%. Diffuse *Eba-h* expression

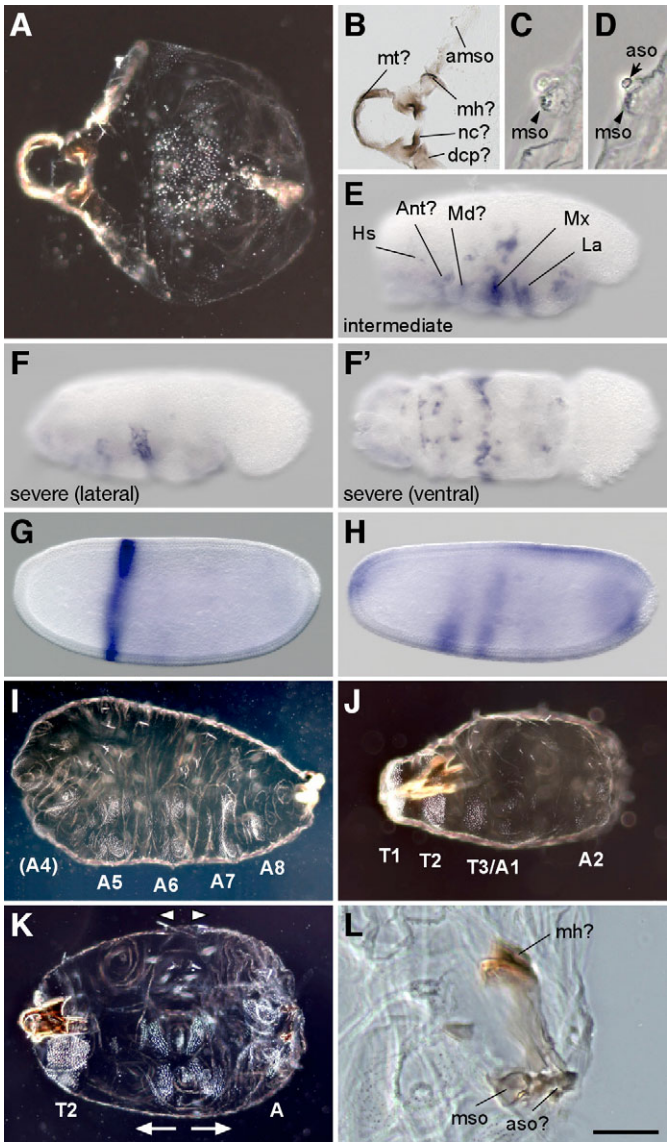

Fig. 7. Functional analysis of *Eba-cad*. (**A-H**) Strong *Eba-cad* RNAi phenotypes. (A) Cuticle in ventral view. (B-D) Magnified head structures. (E-F′) Representative Engrailed patterns in embryos of an intermediate (E) and a strong phenotype (F,F′). (G,H) Representative *Eba-eve* (G) and *Eba-h* (H) expression patterns in blastoderm embryos during cellularization. (**I,J**) Cuticular phenotypes after double-injection of *Eba-cad* mRNA at 0% and ~25% EL (I) or single injection at the posterior pole (100% EL; J). (**K**,**L**) Cuticle showing a strong phenotype after double RNAi against *Eba-cad* and *Eba-nos* (K). Note mid-ventral symmetry plane (arrows) with a reversal of denticle polarity (arrowheads) and abdominal denticles (A), as well as sclerotized material and anterior sense organs at the posterior pole (L). Anterior is towards the left. Views are lateral (E-J), ventral (A-D,F′,K,L) and dorsal (G′,H′). Ant, antennal segment; amso, antennomaxillary complex; aso, antennal sense organ; dcp, dorsal cephalopharyngeal plate; La, labial segment; Md, mandibular segment; Mx, maxillar segment; mh, mouth hooks; mso, maxillary sense organ; mt, median tooth; nc, neck clasps. Scale bar in L: 100 μm for A,B; 31 μm for C,D; 187 μm for E-F′; 178 μm for G,H; 205 μm for I; 160 μm for J; 155 μm for K; 35 μm for L.

was observed in parts of the serosa anlage and in posterior blastoderm, which, judging by a proctodeum-like ventral invagination at about 65% EL, appeared to be excluded from older embryos. In summary, *Eba-cad* is required for proper segmentation in parts of the gnathocephalon and for specifying thoracic and abdominal segments.

To test whether *Eba-cad* was sufficient to induce posterior segmentation, we performed gain-of-function experiments with capped mRNA of *Eba-cad*. As in the case of *Eba-cad* RNAi, only few embryos developed a cuticle after *Eba-cad* mRNA injection at the anterior pole (see Fig. S6D in the supplementary material). In 35% of the cuticles (n=18), head, thorax and abdominal segments A1-A4 were lost (Fig. 7I), 35% exhibited a less severe phenotype, with A3, A4, parts of T1 and some head structures still present, and 30% were indistinguishable from wild type. Following *Eba-cad* mRNA injection at the posterior pole, the resulting cuticles exhibited severe abdominal defects (Fig. 7J; see Fig. S6E in the supplementary material). In one of these cuticles, the entire abdomen was missing, whereas 72% lacked at least abdominal segments A5-A8 (n=29). In addition, we noticed in some of the cuticles defects in T3. Thus, *Eba-cad* is sufficient to repress head development, and both increase or decrease of *Eba-cad* expression in the remaining embryo interferes with segmentation. These results suggest that tightly controlled differential activity levels of *Eba-cad* are essential for polarity and segmentation of the entire *Episyrphus* embryo.

To test whether *Eba-cad* and *Eba-nos* are sufficient to determine overall AP polarity of the embryo, we injected mRNA of both genes together at the anterior pole, but these embryos did not survive. Double RNAi against the mRNAs of both genes resulted in cuticles that were mostly indistinguishable from *Eba-cad* RNAi cuticles (n=20). However, two of the cuticles differed from *Eba-cad* RNAi cuticles: their medioventral denticle field had a symmetry plane indicative of reversed planar polarity in the epidermis, and their posterior ends contained structures reminiscent of mouth hooks and maxillary sense organs (Fig. 7K,L). These cuticles suggest that some head-inducing activity may unfold at the posterior pole of severely shortened embryos when both *Eba-nos* and *Eba-cad* are downregulated.

DISCUSSION

The *Episyrphus* embryo relies heavily on the precise regulation of *Eba-cad*

We found that AP axis specification in *Episyrphus* is strongly dependent on *Eba-cad*. Throughout the embryo, ectopic *Eba-cad* expression interferes with segmentation and differentiation, whereas loss of *Eba-cad* activity interferes with the formation of all but the anterior head segments. In *Drosophila*, ectopic translation of the ubiquitous maternal *caudal* mRNA causes temperature-dependent head involution defects (Niessing et al., 2002; Niessing et al., 1999; Niessing et al., 2000). Ubiquitous expression of a *caudal* transgene in the syncytial blastoderm also causes head involution defects and, in addition, leads to variable fusions of adjacent segment pairs along the entire embryo (Mlodzik et al., 1990). The much stronger gain-of-function phenotype of *caudal* in *Episyrphus* could reflect differences in the experimental designs that were employed. However, loss-of-function experiments also suggest that embryonic development in *Episyrphus* relies more heavily on *Eba-cad* than embryonic development in *Drosophila* does on *caudal*. In *Episyrphus*, *Eba-cad* RNAi suppresses the formation of all but one of the seven *Eba-eve* stripes and severely affects or deletes most postoral segments, whereas *caudal*-deficient *Drosophila* embryos form four out of the seven *even-skipped* stripes and show segmentation in the head, thorax and even parts of the abdomen (Macdonald and Struhl, 1986; Olesnicky et al., 2006). The comparatively weak dependence of AP axis specification

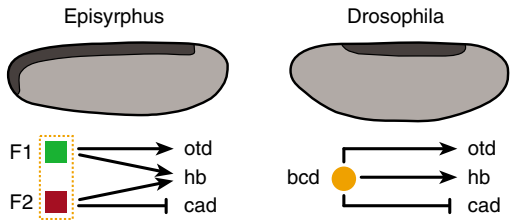

Fig. 8. Model of genetic factors and interactions that determine anterior development in *Episyrphus*. Factor 1 (F1) includes anteriorly enriched Nanos-responsive mRNA and controls the activation of *Eba-otd* (0-30% EL) and early (pre-cellularization) *Eba-hb* (0-90% EL) transcription. Factor 2 (F2) does not respond to ectopic *Eba-nos* activity and mediates restricted zygotic expression of *Eba-hb* (0-30% EL) and *Eba-cad* (20-100% EL). Factor 2 is sufficient to repress posterior development at the anterior pole. In *Drosophila*, the functions of Factor 1 and 2 are both performed by *bicoid*.

in *Drosophila* on *caudal* can be explained by compensatory input from the anterior gradients of *bicoid* and maternal *hunchback* (Hülskamp et al., 1990). In turn, the high *caudal*-dependence of AP axis-specification in *Episyrphus*, which is similarly observed in species that lack the *bicoid* gene such as *Nasonia* (Olesnicky et al., 2006), *Tribolium* (Copf et al., 2004) and the cricket *Gryllus* (Shinmyo et al., 2005), might reflect the absence of maternal *hunchback* and/or *bicoid* activities in this species.

Sources of AP polarity in the *Episyrphus* embryo

Although endogenous *Eba-nos* appeared to be dispensable for AP axis specification, we were able to use ectopic *Eba-nos* expression in gain-of-function experiments as a functional tool to reveal differences in anterior pattern formation between *Episyrphus* and *Drosophila*. *Drosophila* embryos that ectopically express *nanos* at the anterior pole develop a mirror-image duplication of the posterior abdomen (Gavis and Lehmann, 1992; Simpson-Brose et al., 1994). This effect is due to the translational repression of maternal *bicoid* and *hunchback* mRNAs, which control all aspects of anterior development (see Introduction). Both genes contain functionally important NREs, although in wild-type embryos Nanos appears to be irrelevant for the regulation of *bicoid* (Gamberi et al., 2002; Wharton and Struhl, 1991). In *Episyrphus*, we did not observe any trace of abdominal development at the anterior pole after ectopic expression of *Eba-nos*, although the activity was high enough to completely suppress the formation of all but the most posterior segments (A6-A8). This phenotype would be expected if at least two independent factors determine anterior development in *Episyrphus*, only one of which is targeted by ectopic anterior *Eba-nos* activity, whereas the second factor prevents the formation of ectopic posterior structures. We propose that the first factor (Factor 1) consists of an anteriorly enriched NRE-containing mRNA that encodes a protein for the early zygotic activation of *Eba-otd* and *Eba-hb*, and that the second factor (Factor 2), which is not repressed by ectopic *Eba-nos* activity, mediates the repression of *Eba-cad* and part of the anterior *Eba-hb* activation (Fig. 8). Factor 2 appears to function independently of the terminal system, as neither *Eba-cad* nor *Eba-hb* display altered anterior expression domains following RNAi against the putative *torso* homolog of *Episyrphus* (S.L. and U.S.-O., unpublished). Candidate genes for Factor 1 could possibly be identified by searching for NRE-containing sequences in an early embryonic *Episyrphus* EST database.

In summary, AP polarity of the *Episyrphus* embryo appears to be determined by two distinct factors at the anterior pole. We cannot exclude that one of these factors shares homology with *bicoid*, but in any case our model differs significantly from AP axis specification in *Drosophila*, where a single protein, Bicoid, activates *orthodenticle* and *hunchback*, and represses *caudal*. Furthermore, the *Episyrphus* model differs from the *Nasonia* model in that the transcripts of *Eba-otd* and *Eba-gt* (the putative *Episyrphus* ortholog of *giant*; S.L., unpublished data) are of zygotic origin and not localized.

Primitive features of *Episyrphus* development

Episyrphus shares various traits of early embryonic development with non-cyclorrhaphan rather than other cyclorrhaphan flies. It features an anterodorsal serosa anlage, strong influence of *caudal* on the AP axis, a (nearly) ubiquitous early zygotic activation of *hunchback*, as well as *hunchback* expression in the serosa anlage, which has been reported for non-cyclorrhaphan insects (Goltsev et al., 2004; Pultz et al., 2005; Rohr et al., 1999; Wolff et al., 1995) and is absent in *Drosophila*, *Musca* and *Megaselia* (Sommer and Tautz, 1991; Stauber et al., 2000; Tautz and Pfeifle, 1989). During late embryonic development, Engrailed expression in the hindgut of *Episyrphus* embryos is narrow and ring-shaped (S.L. and U.S.-O., unpublished data) similar to some non-cyclorrhaphan insects, whereas Engrailed expression in the hindgut of other cyclorrhaphans is much broader and restricted to the dorsal half (Schmidt-Ott et al., 1994). Based on the primitive features of *Episyrphus* development, we speculate that the ancestral cyclorrhaphan mechanism of AP axis specification was retained in the *Episyrphus* lineage. The restriction of the serosa anlage to dorsal blastoderm in response to increased *Eba-otd* activity might therefore indicate the evolutionary mechanism that altered the position of the serosa anlage.

We thank Michael Stauber for allowing us to use unpublished sequence data and comments on the manuscript, Chip Ferguson for the pSP35 expression vector, Annette Lemke for help with the *Episyrphus* culture, and Benjamin Krinsky for improving the English. Funding was provided by NSF grant 0719445 and by an award of the Faculty Research Fund of the Biological Science Division at the University of Chicago to U.S-O. S.L. was the recipient of a Boehringer Ingelheim Fellowship.

Supplementary material

Supplementary material for this article is available at
http://dev.biologists.org/cgi/content/full/136/1/117/DC1

References

Amaya, E., Musci, T. J. and Kirschner, M. W. (1991). Expression of a dominant negative mutant of the FGF receptor disrupts mesoderm formation in *Xenopus* embryos. *Cell* **66**, 257-270.

Berman, B. P., Nibu, Y. D., P. B., Tomancak, P., Celniker, S. E., Levine, M., Rubin, G. M. and Eisen, M. B. (2002). Exploiting transcription factor binding site clustering to identify cis-regulatory modules involved in pattern formation in the *Drosophila* genome. *Proc. Natl. Acad. Sci. USA* **99**, 757-762.

Brent, A., Yucel, G., Small, S. and Desplan, C. (2007). Permissive and instructive anterior patterning rely on mRNA localization in the wasp embryo. *Science* **315**, 1841-1843.

Brown, S., Fellers, J., Shippy, T., Denell, R., Stauber, M. and Schmidt-Ott, U. (2001). A strategy for mapping *bicoid* on the phylogenetic tree. *Curr. Biol.* **11**, R43-R44.

Bullock, S. L., Stauber, M., Prell, A., Hughes, J. R., Ish-Horowicz, D. and Schmidt-Ott, U. (2004). Differential cytoplasmic mRNA localization adjusts pair-rule transcription factor activity to cytoarchitecture in dipteran evolution. *Development* **131**, 4251-4261.

Cho, P. F., Poulin, F., Andrew Cho-Park, Y. A., Cho-Park, I. B., Chicoine, J. D., Lasko, P. and Sonenberg, N. (2005). A new paradigm for translational control: inhibition via 5′-3′ mRNA tethering by Bicoid and the eIF4E cognate 4EHP. *Cell* **121**, 411-423.

Collins, K. P. and Wiegmann, B. M. (2002). Phylogenetic relationships of the lower Cyclorrhapha (Diptera: Brachycera) based on 28S rDNA sequences. *Insect Syst. Evol.* **33**, 445-456.

Copf, T., Schröder, R. and Averof, M. (2004). Ancestral role of *caudal* genes in axis elongation and segmentation. *Proc. Natl. Acad. Sci. USA* **101**, 17711-17716.
Davis, G. and Patel, N. (2002). Short, long, and beyond: molecular and embryological approaches to insect segmentation. *Annu. Rev. Entomol.* **47**, 669-699.
Driever, W. and Nüsslein-Volhard, C. (1988a). The Bicoid protein determines position in the *Drosophila* embryo in a concentration-dependent manner. *Cell* **54**, 95-104.
Driever, W. and Nüsslein-Volhard, C. (1988b). A gradient of *bicoid* protein in Drosophila embryos. *Cell* **54**, 83-93.
Driever, W. and Nüsslein-Volhard, C. (1989). The *bicoid* protein is a positive regulator of *hunchback* transcription in the early *Drosophila* embryo. *Nature* **337**, 138-143.
Driever, W., Siegel, V. and Nüsslein-Volhard, C. (1990). Autonomous determination of anterior structures in the early *Drosophila* embryo by the *bicoid* morphogen. *Development* **109**, 811-820.
Falciani, F., Hausdorf, B., Schröder, R., Akam, M., Tautz, D., Denell, R. and Brown, S. (1996). Class 3 Hox genes in insects and the origin of *zen*. *Proc. Natl. Acad. Sci. USA* **93**, 8479-8484.
Finkelstein, R. and Perrimon, N. (1990). The *orthodenticle* gene is regulated by *bicoid* and *torso* and specifies *Drosophila* head development. *Nature* **346**, 485-488.
Gamberi, C., Peterson, D. S., He, L. and Gottlieb, E. (2002). An anterior function for the *Drosophila* posterior determinant Pumilio. *Development* **129**, 2699-2710.
Gao, Q. and Finkelstein, R. (1998). Targeting gene expression to the head: the *Drosophila orthodenticle* gene is a direct target of the Bicoid morphogen. *Development* **125**, 4185-4193.
Gao, Q., Wang, Y. and Finkelstein, R. (1996). *Orthodenticle* regulation during embryonic head development in *Drosophila*. *Mech. Dev.* **56**, 3-15.
Gavis, E. R. and Lehmann, R. (1992). Localization of *nanos* RNA controls embryonic polarity. *Cell* **71**, 301-313.
Goltsev, Y., Hsiong, W., Lanzaro, G. and Levine, M. (2004). Different combinations of gap repressors for common stripes in *Anopheles* and *Drosophila* embryos. *Dev. Biol.* **275**, 435-446.
Grimaldi, D. and Engel, M. S. (2005). *Evolution of Insects*. Cambridge: Cambridge University Press.
Hartenstein, V. (1993). Atlas of *Drosophila* Development. Cold Spring Harbor, NY: Cold Spring Harbor Laboratory Press.
Hülskamp, M., Schroeder, C., Pfeifle, C., Jaeckle, H. and Tautz, D. (1989). Posterior segmentation of the *Drosophila* embryo in the absence of a maternal posterior organizer gene. *Nature* **338**, 629-632.
Hülskamp, M., Pfeifle, C. and Tautz, D. (1990). A morphogenetic gradient of Hunchback protein organizes the expression of the gap genes *Krüppel* and *knirps* in the early *Drosophila* embryo. *Nature* **346**, 577-580.
Irish, V., Lehmann, R. and Akam, M. (1989). The *Drosophila* posterior-group gene *nanos* functions by repressing *hunchback* activity. *Nature* **338**, 646-648.
Kosman, D., Mizutani, C. M., Lemons, D., Cox, W. G., McGinnis, W. and Bier, E. (2004). Multiplex detection of RNA expression in *Drosophila* embryos. *Science* **305**, 846.
Lemke, S. J., Stauber, M., Shaw, P. J., Rafiqi, A. M., Prell, A. and Schmidt-Ott, U. (2008). *bicoid* occurrence and Bicoid-dependent *hunchback* regulation in lower cyclorrhaphan flies. *Evol. Dev.* **10**, 413-420.
Lynch, J. A., Olesnicky, E. C. and Desplan, C. (2006). Regulation and function of *tailless* in the long germ wasp *Nasonia vitripennis*. *Dev. Genes Evol.* **216**, 493-498.
Macdonald, P. M. and Struhl, G. (1986). A molecular gradient in early *Drosophila* embryos and its role in specifying the body pattern. *Nature* **324**, 537-545.
Mlodzik, M., Gibson, G. and Gehring, W. J. (1990). Effects of ectopic expression of *caudal* during *Drosophila* development. *Development* **109**, 271-277.
Moulton, J. K. and Wiegmann, B. M. (2004). Evolution and phylogenetic utility of CAD (rudimentary) among Mesozoic-aged Eremoneuran Diptera (Insecta). *Mol. Phylogenet. Evol.* **31**, 363-378.
Murata, Y. and Wharton, R. P. (1995). Binding of *pumilio* to maternal *hunchback* mRNA is required for posterior patterning in *Drosophila* embryos. *Cell* **80**, 747-756.
Negre, B., Casillas, S., Suzanne, M., Sanchez-Herrero, E., Akam, M., Nefedov, M., Barbadilla, A., de Jong, P. and Ruiz, A. (2005). Conservation of regulatory sequences and gene expression patterns in the disintegrating *Drosophila* Hox gene complex. *Genome Res.* **15**, 692-700.
Niessing, D., Dostatni, N., Jäckle, H. and Rivera-Pomar, R. (1999). Sequence interval within the PEST domain of Bicoid is important for translational repression of *caudal* mRNA in the anterior region of the *Drosophila* embryo. *EMBO J.* **18**, 1966-1973.
Niessing, D., Driever, W., Sprenger, F., Taubert, H., Jäckle, H. and Rivera-Pomar, R. (2000). Homeodomain position 54 specifies transcriptional versus translational control by Bicoid. *Mol. Cell* **5**, 395-401.
Niessing, D., Blanke, S. and Jäckle, H. (2002). Bicoid associates with the 5′-cap-bound complex of *caudal* mRNA and represses translation. *Genes Dev.* **16**, 2576-2582.
Ochoa-Espinosa, A., Yucel, G., Kaplan, L., Pare, A., Pura, N., Oberstein, A., Papatsenko, D. and Small, S. (2005). The role of binding site cluster strength in Bicoid-dependent patterning in *Drosophila*. *Proc. Natl. Acad. Sci. USA* **102**, 4960-4965.
Olesnicky, E. C., Brent, A. E., Tonnes, L., Walker, M., Pultz, M. A., Leaf, D. and Desplan, C. (2006). A *caudal* mRNA gradient controls posterior development in the wasp *Nasonia*. *Development* **133**, 3973-3982.
Patel, N. H., Martin-Blanco, E., Coleman, K. G., Poole, S. J., Ellis, M. C., Kornberg, T. B. and Goodman, C. S. (1989). Expression of *engrailed* proteins in arthropods, annelids and chordates. *Cell* **58**, 955-968.
Posada, D. and Crandall, K. A. (1998). MODELTEST: testing the model of DNA substitution. *Bioinformatics* **14**, 817-818.
Pultz, M. A., Pitt, J. N. and Alto, N. M. (1999). Extensive zygotic control of the anteroposterior axis in the wasp *Nasonia vitripennis*. *Development* **126**, 701-710.
Pultz, M. A., Westendorf, L., Gale, S. D., Hawkins, K., Lynch, J., Pitt, J. N., Reeves, N. L., Yao, J. C. Y., Small, S., Desplan, C. et al. (2005b). A major role for zygotic *hunchback* in patterning the *Nasonia* embryo. *Development* **132**, 3705-3715.
Rafiqi, A. M., Lemke, S. J., Ferguson, S., Stauber, M. and Schmidt-Ott, U. (2008). Evolutionary origin of the amnioserosa in cyclorrhaphan flies correlates with spatial and temporal expression changes of *zen*. *Proc. Natl. Acad. Sci. USA* **105**, 234-239.
Rohr, K. B., Tautz, D. and Sander, K. (1999). Segmentation gene expression in the mothmidge *Clogmia albipunctata* (Diptera, Psychodidae) and other primitive dipterans. *Dev. Genes Evol.* **209**, 145-154.
Roth, S. (2004). Gastrulation in other insects. In *Gastrulation* (ed. C. D. Stern), pp. 105-121. Cold Spring Harbor, NY: Cold Spring Harbor Laboratory Press.
Schmidt-Ott, U. (2005). Insect serosa: a headline in comparative developmental genetics. *Curr. Biol.* **15**, R245-R247.
Schmidt-Ott, U. and Technau, G. M. (1992). Expression of *en* and *wg* in the embryonic head and brain of *Drosophila* indicates a refolded band of seven segment remnants. *Development* **116**, 111-125.
Schmidt-Ott, U., Sander, K. and Technau, G. M. (1994). Expression of *engrailed* in embryos of a beetle and five dipteran species with special reference to the terminal regions. *Roux's Arch. Dev. Biol.* **203**, 298-303.
Schröder, R. (2003). The genes *orthodenticle* and *hunchback* substitute for *bicoid* in the beetle *Tribolium*. *Nature* **422**, 621-625.
Schroeder, M. D., Pearce, M., Fak, J., Fan, H.-Q., Unnerstall, U., Emberly, E., Rajewsky, N., Siggia, E. D. and Gaul, U. (2004). Transcriptional control in the segmentation gene network of *Drosophila*. *PLOS* **2**, e271.
Schulz, C., Schröder, R., Hausdorf, B., Wolff, C. and Tautz, D. (1998). A *caudal* homologue in the short germ band beetle *Tribolium* shows similarities to both, the Drosophila and the vertebrate *caudal* expression patterns. *Dev. Genes Evol.* **208**, 283-289.
Segal, E., Raveh-Sadka, T., Schroeder, M., Unnerstall, U. and Gaul, U. (2008). Predicting expression patterns from regulatory sequence in *Drosophila* segmentation. *Nature* **451**, 535-540.
Shimodaira, H. and Hasegawa, M. (2001). CONSEL: for assessing the confidence of phylogenetic tree selection. *Bioinformatics* **17**, 1246-1247.
Shinmyo, Y., Mito, T., Matsushita, T., Sarashina, I., Miyawaki, K., Ohuchi, H. and Noji, S. (2005). *caudal* is required for gnathal and thoracic patterning and for posterior elongation in the intermediate-germband cricket *Gryllus bimaculatus*. *Mech. Dev.* **122**, 231-239.
Simpson-Brose, M., Treisman, J. and Desplan, C. (1994). Synergy between the *hunchback* and *bicoid* morphogens is required for anterior patterning in *Drosophila*. *Cell* **78**, 855-865.
Sommer, R. and Tautz, D. (1991). Segmentation gene expression in the housefly *Musca domestica*. *Development* **113**, 419-430.
Sonoda, J. and Wharton, R. P. (1999). Recruitment of Nanos to *hunchback* mRNA by Pumilio. *Genes Dev.* **13**, 2704-2712.
Sonoda, J. and Wharton, R. P. (2001). *Drosophila* Brain Tumor is a translational repressor. *Genes Dev.* **15**, 762-773.
St Johnston, D. and Nüsslein-Volhard, C. (1992). The origin of pattern and polarity in the *Drosophila* embryo. *Cell* **68**, 201-220.
Stauber, M., Taubert, H. and Schmidt-Ott, U. (2000). Function of *bicoid* and *hunchback* homologs in the basal cyclorrhaphan fly *Megaselia* (Phoridae). *Proc. Natl. Acad. Sci. USA* **97**, 10844-10849.
Stauber, M., Prell, A. and Schmidt-Ott, U. (2002). A single *Hox3* gene with composite *bicoid* and *zerknüllt* expression characteristics in non-Cyclorrhaphan flies. *Proc. Natl. Acad. Sci. USA* **99**, 274-279.
Stauber, M., Lemke, S. and Schmidt-Ott, U. (2008). Expression and regulation of *caudal* in the lower cyclorrhaphan fly *Megaselia*. *Dev. Genes Evol.* **218**, 81-87.
Stern, D. L. and Sucena, E. (2000). Preparation of larval and adult cuticles for light microscopy. In *Drosophila Protocols* (ed. W. Sullivan, M. Ashburner and R. S. Hawley), pp. 601-615. Cold Spring Harbor, NY: Cold Spring Harbor Laboratory Press.

Struhl, G. (1989). Differing strategies for organizing anterior and posterior body pattern in *Drosophila* embryos. *Nature* **338**, 741-744.
Struhl, G., Struhl, K. and Macdonald, P. M. (1989). The gradient morphogen *bicoid* is a concentration-dependent transcriptional activator. *Cell* **57**, 1259-1273.
Surkova, S., Kosman, D., Kozlov, K., Manu Myasnikova, E., Samsonova, A. A., Spirov, A., Vanario-Alonso, C. E., Samsonova, M. and Reinitz, J. (2008). Characterization of the *Drosophila* segment determination morphome. *Dev. Biol.* **313**, 844-862.
Swofford, D. L. (2002). PAUP*. Phylogenetic analysis using parsimony (* and other methods). Sunderland, MA: Sinauer Associates.
Tautz, D. (1988). Regulation of the *Drosophila* segmentation gene *hunchback* by two maternal morphogenetic centers. *Nature* **332**, 281-284.
Tautz, D. and Pfeifle, C. (1989). A non-radioactive in situ hybridization method for the localization of specific RNAs in *Drosophila* embryos reveals translational control of the segmentation gene *hunchback*. *Chromosoma* **98**, 81-85.
Tautz, D., Lehmann, R., Schnürch, H., Schuh, R., Seifert, E., Kienlin, A., Jones, K. and Jäckle, H. (1987). Finger protein of novel structure encoded by *hunchback*, a second member of the gap class of *Drosophila* segmentation genes. *Nature* **327**, 383-389.
Tautz, D., Friedrich, M. and Schröder, R. (1994). Insect embryogenesis: what is ancestral and what is derived? *Development* **Suppl.** 193-199.
Vardy, L. and Orr-Weaver, T. L. (2007). Regulating translation of maternal messages: multiple repression mechanisms. *Trends Cell Biol.* **17**, 547-554.
Wharton, R. P. and Struhl, G. (1991). RNA regulatory elements mediate control of *Drosophila* body pattern by the posterior morphogen *nanos*. *Cell* **67**, 955-968.
Wolff, C., Sommer, R., Schröder, R., Glaser, G. and Tautz, D. (1995). Conserved and divergent expression aspects of the *Drosophila* segmentation gene *hunchback* in the short germ band embryo of the flour beetle *Tribolium*. *Development* **121**, 4227-4236.
Yeates, D. K. and Wiegmann, B. M. (2005). Phylogeny and evolution of Diptera: recent insights and new perspectives. In *The evolutionary Biology of Flies* (ed. D. K. Yeates and B. M. Wiegmann), pp. 14-44. New York: Columbia University Press.
Zdobnov, E. M., von Mering, C., Letunic, I., Torrents, D., Suyama, M., Copley, R. R., Christophides, G. K., Thomasova, D., Holt, R. A., Subramanian, G. M. et al. (2002). Comparative genome and proteome analysis of *Anopheles gambiae* and *Drosophila melanogaster*. *Science* **298**, 149-159.